ELSEVIER

Colloids and Surfaces
A: Physicochemical and Engineering Aspects 179 (2001) 57–64

COLLOIDS AND SURFACES A

www.elsevier.nl/locate/colsurfa

Tethers connecting daughter vesicles and parent red blood cell may be formed due to ordering of anisotropic membrane constituents

Veronika Kralj-Iglič [a,*], Aleš Iglič [b], Malgorzata Bobrowska-Hägerstrand [c], Henry Hägerstrand [c]

[a] *Faculty of Medicine, Institute of Biophysics, University of Ljubljana, Lipičeva 2, SI-1000 Ljubljana, Slovenia*
[b] *Laboratory of Applied Physics, Faculty of Electrical Engineering, University of Ljubljana, Ljubljana, Slovenia*
[c] *Department of Biology, Åbo Akademi University, Åbo/Turku, Finland*

Received 13 December 1999; accepted 25 July 2179

Abstract

Vesiculation of red blood cells at high alkaline pH was studied experimentally and theoretically. It was observed that the red blood cell daughter vesicles can be connected to the parent cell by thin tubes (tethers). It is shown theoretically that the formation of tethers may be energetically favourable due to the quadrupolar ordering of the anisotropic membrane constituents in the strong curvature field of the tethers.

Keywords: Red blood cell; High pH; Membrane inclusions; Tether; Orientation

1. Introduction

The cell membrane is composed of a phospholipid bilayer in which proteins are embedded. At a given volume, the cell shape of a mature mammalian red blood cell, which does not contain internal structures, is determined solely by the properties of its membrane [1]. Red blood cell shape transformations are therefore a convenient system for observation of the changes in membrane features and interactions between the membrane and the surrounding solution. Analoguously, these features can be studied on an even simpler system — phospholipid vesicles. Both systems can therefore be subject to the similar general principles, although it should be taken into account that in red blood cells, the phospholipid bilayer contains embedded proteins and is underlaid by the membrane skeleton [2].

It was observed in giant phospholipid vesicles that after being formed, the vesicles are often connected to each other by narrow tubular structures of different lengths [3,4]. These thin tubes

* Corresponding author. Tel.: +386-1-5437620; fax: +386-1-1315127.
E-mail address: vera.kralj-iglic@biofiz.mf.uni-lj.si (V. Kralj-Iglič).

0927-7757/01/$ - see front matter
PII: S0927-7757(00)00721-4

are called tethers. It was indicated [3] that tethers are difficult to visualise and are also very fragile so that they may have been overlooked in biological systems, although they could have an important role in the function of the Golgi system and other transport systems involving vesicles. Tethers have been reported to occur also in red blood cells [5,6], but visual evidence for their occurrence seems to be lacking.

Morphological features, such as exvaginations and invaginations can be observed in different cell types. For example, long cylindrical protrusions, as well as spherical exovesicles, were observed in vesiculating cancer cells [7], where the integrity of the cytoskeleton and its interaction with the membrane were abolished.

In this work, we report on the experiment in which we induced occurence of exovesicles by incubating the red blood cells in high pH buffer. We observed that the daughter vesicles were often connected to the parent cell by tethers. We propose a possible explanation for the stability of the tethers, based on the orientational and distributional effects of the anisotropic membrane constituents.

2. Experiment

2.1. Material and methods

Blood was drawn from the authors by venipuncture into heparinized tubes. The red blood cells were washed three times in a buffer containing Hepes 10 mM, NaCl 128 mM, KCl 3 mM (pH 7.4) and subsequently suspended in the buffer at a cell density of 1.65×10^9 cells/ml. A few microlitres of the red blood cell stock suspension was pipetted into Eppendorf tubes containing 100 μl of the buffer at pH $\simeq$ 12. In some samples, dibucaine (100 μM) was added following 10–60 min incubation. Incubation was carried out at room temperature under gentle mixing. Aliquots of the sample were studied by phase contrast microscopy while hanging in a drop under a cover glass. Samples were fixed by glutaraldehyde (final conc. 1%) before being photographed by Nomarski interference contrast microscopy.

2.2. Experimental results

Incubation of red blood cells, originally suspended in the buffer at pH 7.4, in the high pH buffer (pH $\simeq$ 12) resulted in an echinocytogenic shape alteration, where largely spherical cell shapes (sphero-echinocytes) were attained. During this process, microexovesicles were apparently shed from the cells, as evidenced from TEM micrographs showing microexovesicles in the suspension (not shown). As incubation continued, an additional or alternative vesiculation occured at approximately pH 9.5 [6,8]. Small vesicles — large enough to be visible by light microscopy — were formed. The release of such vesicles was accelerated by the addition of dibucaine, a cationic phenothiazine (which is at neutral pH stomatocytogenic). Such vesicles released from the mother cell are shown in Fig. 1. It was observed that these vesicles may be connected to the parent cell by a thin tether (strand/stalk). Typically, the vesicles connected to the parent cell with tethers were distributed around the parent cell as in Fig. 1 and moved synchroneously with the parent cell. Unfortunately, we did not succeed in preserving the barely visible tether structures for light- or electron-microscopy studies. A fragmentation of the erythrocyte into very large vesicles often occurred (Fig. 2) before the hemolytic collapse. The large vesicle in Fig. 2 is connected to the mother cell with a thick tether. The observed pH-induced shape alterations and their time course depended on factors affecting the increase of intracellular pH, e.g. the initial pH of the incubation media and the amount of cells added (i.e. their buffering capacity).

3. Theory

3.1. Model

The stable (equilibrium) shape of the red blood cell is determined by the minimum of the membrane free energy. In minimization of the membrane free energy it is taken into account that the membrane area and the cell volume are kept constant.

We visualize the membrane as composed of a continuum of phospholipid molecules, in which laterally mobile proteins are embedded. Accordingly, the membrane is described as an elastic continuum decorated with inclusions. The inclusion is the complex composed of the protein and phospholipid molecules that are significantly distorted in order to adjust to the shape of the protein [9,10] or a lipid complex [11–13].

To describe the cell shape we take as the base the bilayer couple model [14,15]. The membrane free energy consists of the elastic energy of the membrane continuum W_{el} and the free energy of the inclusions F_m,

$$F = W_b + F_m. \tag{1}$$

The bending energy of the membrane W_b is [16]

$$W_b = \frac{k_c}{2}\int (2\bar{C} - C_0)^2 \, dA + k_G \int K \, dA, \tag{2}$$

where k_c and k_G are the membrane local and Gaussian bending constants, respectively, $\bar{C} = (C_1 + C_2)/2$ is the mean curvature of the membrane, $K = C_1C_2$ is the Gaussian curvature of the membrane, C_1 and C_2 are the principal curvatures of the membrane, C_0 is the spontaneous curvature of the membrane and dA is the area element of the membrane. The integration is performed over the membrane area A. While the first term in Eq. (2) determines the cell shape [1], the contribution of the second term is constant within a given topology of the system. In our case, the cell membrane remains closed so that the topology of the cell shape is unchanged upon the cell shape transformation. Therefore the Gaussian term does not influence the cell shape.

The free energy of the inclusions is [17]

$$F_m = -kTM_T \ln\left(\frac{1}{A}\int q_c I_0\left(\frac{\xi + \xi^*}{2kT}\hat{C}\hat{C}_m\right) dA\right), \tag{3}$$

where T is the temperature of the system, k is the Boltzmann constant,

$$q_c = \exp\left(-\frac{\xi}{2kT}(\bar{C} - \bar{C}_m)^2 - \frac{\xi + \xi^*}{4kT}(|\hat{C}|^2 + |\hat{C}_m|^2)\right), \tag{4}$$

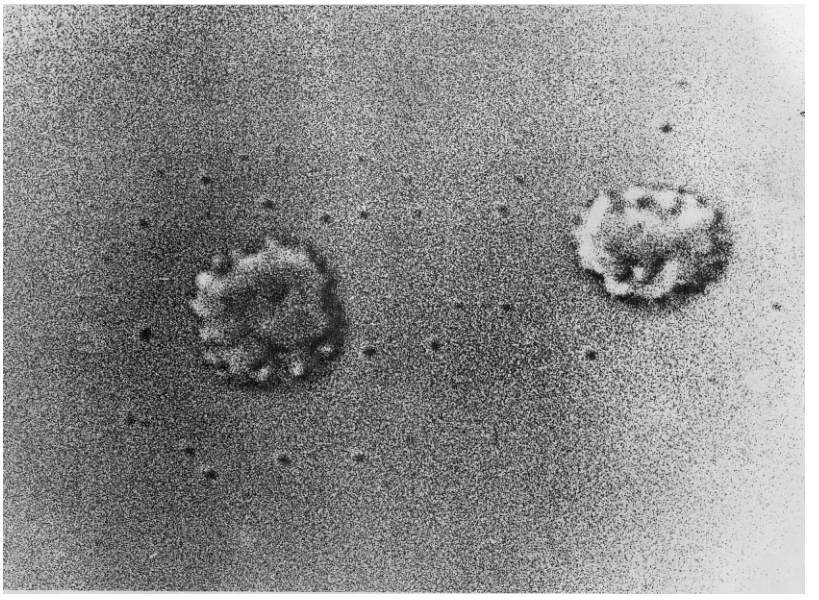

Fig. 1. Vesiculation in human red blood cells. Red blood cells were incubated (20 min, room temperature) in high pH saline (pH $\simeq$ 12) whereafter dibucaine (100 μM, 10 min) was added. Following $\simeq$ 10 min incubation the sample was fixed, applied between object and cover glass and photographed (Nomarski interference contrast). Note the exovesicles located around the parent red blood cells. Tethers are not visible in the figure.

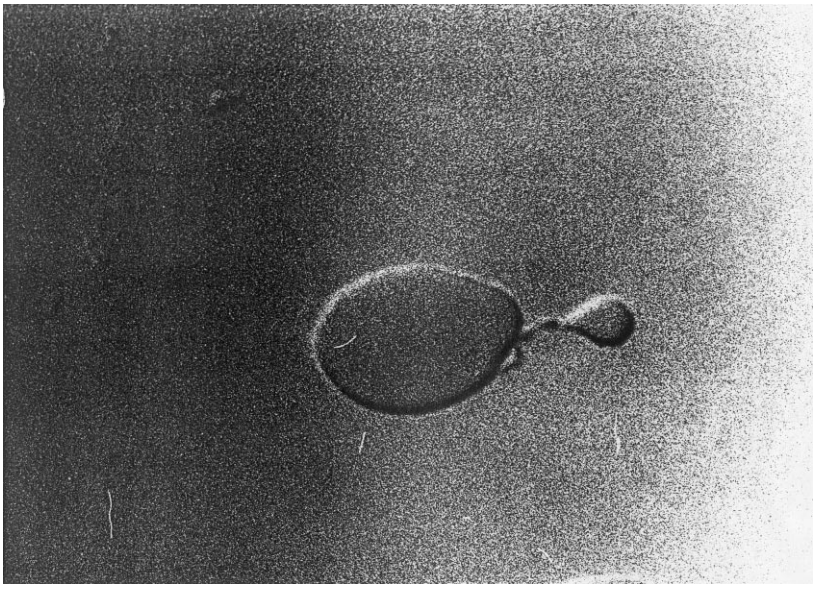

Fig. 2. Vesiculation in human red blood cells. Red blood cells were incubated in high saline pH. For photography (Nomarski interference contrast) red blood cells were applied between object and cover glass. A large vesicle is connected to the parent cell by a tubular structure.

I_0 is the modified Bessel function, ξ and ξ^* are positive interaction constants, $\hat{C}=\frac{1}{2}(C_1-C_2)$, $\bar{C}_m=\frac{1}{2}(C_{1m}+C_{2m})$, $\hat{C}_m=\frac{1}{2}(C_{1m}-C_{2m})$, C_{1m} and C_{2m} are the principal curvatures intrinsic to the inclusion and ω is the orientation of the inclusion with respect to the principal system of the membrane. The inclusion is isotropic if $\hat{C}_m=0$ while if $\hat{C}_m\neq 0$ the inclusion is anisotropic. All inclusions are taken to be equal and indistinguishable.

The free energy of the inclusion derives from the mismatch between the local membrane shape and the intrinsic shape of the inclusion (given by $\bar{C}$, $\hat{C}$ and $\bar{C}_m$, $\hat{C}_m$, respectively and by the relative orientation of the two principal systems ω). It is taken into account that in the equilibrium, the function that describes the lateral distribution of the inclusions over the membrane is an extremal of the functional defined by the membrane free energy and the constraint of the fixed number of the inclusions in the membrane M_T [17]. Therefore, the inclusions are in general nonhomogeneously distributed over the membrane area [10,18–22]. They are accumulated at regions of favourable curvature and depleted from the regions of unfavourable curvature. If the inclusions are anisotropic, they are also oriented according to the local curvature field [17,23].

It was established on the basis of the bilayer couple model [14,15,24] that the difference between the outer and the inner monolayer areas of the red blood cell membrane ($\triangle A$),

$$\triangle A = 2h\int \bar{C}\,\mathrm{d}A, \tag{5}$$

where h is the distance between the two monolayer neutral areas, increases with increasing pH [8,25–27]. To describe this process, we took, as a base, the sequence of shapes of increasing $\triangle A$ starting from an axisymmetrical pear shape and leading to the shape composed of a spherical mother vesicle and a spherical daughter exovesicle. The shapes were obtained by the minimization of the membrane bending energy [28–30]. Upon the increase of ΔA, the neck of the pear shape becomes increasingly pronounced, however, upon further increase of ΔA, the neck area diminishes so that the sequence ends with two spherical vesicles connected by an infinitesimal neck. If the membrane free energy of the anisotropic inclu-

sions is calculated for such sequence of shapes [17], it sharply decreases as the neck narrows, due to the accumulation and orientational ordering of the inclusions in the narrow neck [17]. Upon further increase of ΔA the free energy of the inclusions increases so that the $F_m(\triangle A)$ curve exhibits a sharp minimum [17].

Here, we consider a possibility that the neck might be favourable for the given kind of inclusions, so that it could be expected that upon increase of ΔA from the shape corresponding to the minimum of the membrane free energy within the given sequence, instead of shrinking, the neck would elongate into a tether. To determine the equilibrium shapes in detail, the minimization of the free energy F (Eq. (1)) with respect to the shape would be necessary. However, qualitative behavior of the system can be predicted also by an approximative manner. We simulated growth of the tether by adding to the shape corresponding to the minimum of ΔA a cylinder of the radius of the neck. As the neck is narrow, the contribution of this cylinder to the membrane area and the cell volume is negligible for relatively short tethers that we consider in this work.

To simulate the effect of different kinds of inclusions we calculated the membrane free energy corresponding to the minimum with respect to the shape for different parameters $\bar{C}_m$ and $|\hat{C}_m|$.

3.2. Theoretical results

Fig. 3 shows the membrane free energy and its contributions for the sequence of shapes with increasing area difference. Two different kinds of inclusions (characterized by different $\bar{C}_m$ and $|\hat{C}_m|$ are considered: the inclusions that favour flat regions ($\bar{C}_m = 0$ and $\hat{C}_m = 0$) and the inclusions that favour the regions where ($\bar{C}_m \neq 0$ and $|\hat{C}_m| \neq 0$).

When the inclusions favour flat regions the membrane free energy monotonously increases with increasing area difference (Fig. 3a). The contribution of the inclusions is constant, so that the increase of the free energy is due to the increase of the bending energy (Fig. 3a). The formation of a tether is not favoured due to high bending energy of the tether, therefore the sequence of the equilibrium shapes leads to the limiting shape composed of two spheres. This means that the value of the area difference cannot be further increased within this class of shapes.

When the inclusions favour anisotropic regions with high curvature, the free energy of the inclusions decreases as the neck forms due to orientational ordering of the anisotropic inclusions (Fig.

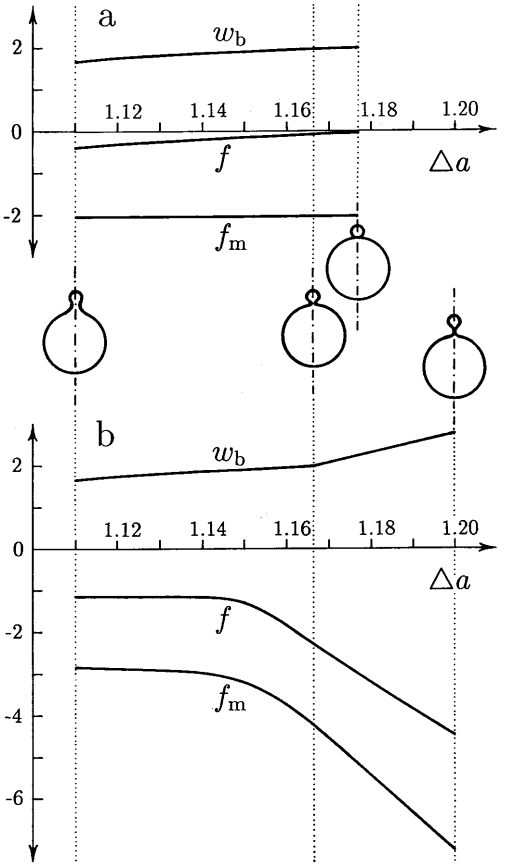

Fig. 3. The relative free energy of the anistropic membrane inclusions $f_m = F_m/8\pi k_c$, the relative membrane bending energy $w_b = W_b/8\pi k_c$ and the relative membrane free energy $f = F/8\pi k_c$ dependence on the relative difference between the membrane layer areas $\triangle a = \triangle A/8\pi R_{sph} h$ in the case that the inclusions favour flat regions $\bar{C}_m = \hat{C}_m = 0$ (a); and in the case that the inclusions favour anisotropic regions that are highly curved $\bar{C}_m R_{sph} = 45$, $\hat{C}_m R_{sph} = 90$ (b). The relative volume is chosen $v = 36\pi\sqrt{V^2/A^3} = 0.95$. The parameters used in calculation are $M_T kT/8\pi k_c = 1$, $\xi = \xi^*$, $\xi/kTR^2_{sph} = 0.001$, where $R_{sph} = (A/4\pi)^{1/2}$. The relative free energy of the inclusions is determined only up to a constant.

3b). If the area difference is further increased, the shapes with the tether have lower membrane free energy than the shapes with shrinking neck. The decrease of the free energy of the inclusions dominates the increase of the membrane bending energy (Fig. 3b). In effect, the membrane free energy decreases with increasing length of the tether (Fig. 3b).

Our results indicate that the formation of the tether connecting the daughter vesicle and the parent cell may be energetically favourable due to ordering and redistribution of the anisotropic membrane inclusions that favour high curvature. As there is always some amount of the anisotropic inclusions in the membrane, the effect is always present. Its importance for the shape is however given in terms of the model constants. For the values of the model parameters we took that the total number of inclusions M_T is of the order of 10^3; the membrane bending constant is $\simeq 10^{-19}$ J [30]; to estimate the constant of the interaction between the inclusion and the surrounding membrane $\xi = \xi^*$, we assumed that the energy cost in distortion of a tail of a phospholipid molecule within the inclusion would be approximately equal as in the difference of the packing between the bilayer and the cylindrical aggregation geometries. Such difference is of the order of (0.1–0.5)kT per tail of the phospholipid molecule [31]. If we take that there are some ten molecules involved in the inclusion, the energy of the inclusion could reach several kT. From this it can be estimated [17] that $\xi/kTR_{sph}^2 \simeq 10^{-3}$, where $R_{sph} \simeq 3$ μm, corresponding to the membrane area about 150 μm^2 [1]. If the total number of the inclusions is smaller, if their anisotropy is weaker and if the width of the tether is larger, the effect of the free energy of the anistropic inclusions is less pronounced.

4. Discussion

To explain the shape alterations induced by high pH in intact red blood cells, several mechanisms were suggested originating form protein–lipid bilayer and skeleton–bilayer interactions as well as from conformational changes of the membrane skeleton and membrane integral proteins [8,27,32,33]. In this work, we suggest that orientational ordering and redistribution of the anisotropic membrane embedded molecules that favour high curvature may significantly decrease the membrane free energy when the tether begins growing. On the basis of these results, we propose that the formation of tethers may be energetically favourable due to the ordering and redistribution of the anisotropic membrane inclusions in the strong curvature field of the tethers.

Although the principle was demonstrated for a given kind of inclusion, it can be generalized to more than one kind as there are many different species of molecules embedded in the membrane. At present, we do not have a definite answer regarding the specification of the anisotropic inclusions. Integral membrane proteins were found in tethers pulled out of a red blood cell membrane by applying an external force [34,35]. There were no membrane skeletal components and no band three proteins in the tethers [35,36]. It was also shown that red blood cell microexovesicles obtained by various methods are depleted in α- and β-spectrin, while lipid and protein composition is different than in the mother cell [37]. The composition of the tether remains a subject of investigation [35]. However, as the membrane constituents are generally not axisymmetric, the anisotropic inclusion may be any such protein with adjacent phospholipid molecules as well as a phospholipid complex [9,10,12,13,32] that constitutes tether.

Another energy term that should be discussed is the energy of the relative stretching of the two membrane monolayers. The energy of the relative stretching W_r forms a quadratic function of ΔA [24,38–40].

$$W_r = \frac{k_r}{2Ah^2}(\triangle A - \triangle A_0)^2, \quad (6)$$

where k_r is the membrane nonlocal bending constant, and $\triangle A_0$ is the area difference of the unstretched monolayers. Including the energy of the relative stretching does not affect the set of the possible shapes obtained by the minimization of any form of energy that includes $\triangle A$ [24,38–40]. The membrane nonlocal bending constant k_r was measured [35], while the value of the parame-

ter $\triangle A_0$ has not yet been systematically determined. Nevertheless, if the value of $\triangle A_0$ is chosen large enough, the minimum of the quadratic function lies far to the right from the region of ΔA of the sequence so that the sum $W_b + W_r$ may monotonously decrease with increasing ΔA. However, the energy of the relative stretching does not depend on the details of the shape, e.g. does not distinguish between the shape with the infinitesimal neck and the shape with a short tether, as long as both shapes have the same ΔA. As the membrane bending energy is lower for the sequence ending with two spheres connected by the infinitesimal neck, the relative stretching can not explain the stability of the tether.

The echinocytic shape at intermediate values of pH is determined also by the membrane cytoskeleton [41–46] which is at normal conditions attached to the membrane [47,48]. The shear energy of the membrane skeleton was shown to influence the stable shape of the red blood cell [41,42,44–46]. However, the interaction between the membrane and the skeleton is abolished at high pH values [49,50], therefore it is assumed that in these conditions the shear energy of the membrane skeleton does not influence the cell shape [8].

The importance of deviatoric bending for the stability of the tubular necks was indicated previously [51,52]. An expression for the membrane free energy was proposed where the free energy density was expanded in terms of two invariants of the curvature tensor: the mean curvature $\bar{C}$ and the curvature deviator $|\hat{C}|$,

$$F = \int \left(2B_s \left(\bar{C} - \frac{C_0}{2} \right)^2 + 2B_a (|\hat{C}| - \vartheta)^2 \right) \mathrm{d}A, \qquad (7)$$

where B_s and B_a are the constants of the isotropic and deviatoric bending, respectively and ϑ is the spontaneous warp [51,52]. The theory used in this work starts from the microscopic scale and provides a clarification of the phenomena based on the orientational ordering of the molecules within the membrane. The deviatoric part of the free energy density Eq. (7) can be recovered from Eq. (3) in the case when the membrane is constantly and strongly anisotropically curved over the entire area. We may say that in this case the anisotropic membrane inclusions produce spontaneous warp. For the closed shapes that have a complex morphology the free energy of the strongly anisotropic inclusions can not be described by means of an integral of the free energy density Eq. (7). We argue that for such shapes the full expression Eq. (3) should be taken into account.

The deviatoric membrane properties induced by anisotropic membrane constituents also provide an explanation for stable tubular structures in other systems [23,53,54], that could not be explained by the models based on the minimization of the membrane bending energy [55].

The erythrocyte membrane has been found to exhibit shape fluctuations [56] which importantly influence lateral ordering of the inclusions of nearly flat membranes [57–60]. As our theoretical analysis does not include the shape fluctuations, we cannot say how the fluctuations affect ordering of the inclusions in tethers. The experimental data, however, indicate that when the limit shape is approached close enough, the fluctuations of the cell body are diminished [61,62]. The experimental data also indicate a high degree of order in thin tubular structures. Ordering of the intramembraneous particles was observed in the spontaneously released tubular microvesicles of in vitro aged sheep erythroctes and ghosts [63]. High in-plane order was also found in the tubular structures made of the phospholipid 1,2-bis(tricosa-10,12-diynoyl)-sn-glycero-3-phosphocholine [64].

In conclusion, we observed that at high pH, the red blood cell daughter vesicles can be connected to the parent cell by tethers. It is shown that the formation of tethers may be energetically favourable due to the ordering of the anisotropic membrane inclusions in the strong curvature field of the tethers.

References

[1] P.B. Canham, J. Theor. Biol. 26 (1970) 61.
[2] T.L. Steck, in: W.D. Stein, F. Brooner (Eds.), Cell Shape. Determinants, Regulation and Regulatory Role, Academic Press, New York, 1989, p. 205.
[3] L. Mathivet, S. Cribier, P.F. Devaux, Biophys. J. 70 (1996) 1112.

[4] H.G. Döbereiner, E. Evans, M. Kraus, U. Seifert, M. Wortis, Phys. Rev. E 55 (1997) 4458.
[5] G. Lelkes, I. Fodor, Biochem. Biophys. Acta 1065 (1991) 135.
[6] M. Bobrowska-Hägerstrand, A. Iglič, H. Hägerstrand, Cell. Mol. Biol. Lett. 2 (1997) 9, available on www.abo.fi/fak/mnf/biol/.
[7] V. Kralj-Iglič, U. Batista, H. Hägerstrand, A. Iglič, J. Majhenc, M. Sok, Radiol. Oncol. 32 (1998) 119.
[8] A. Iglič, H. Hägerstrand, V. Kralj-Iglič, M. Bobrowska-Hägerstrand, J. Biomech. 31 (1998) 151.
[9] S. Marçelja, Biochim. Biophys. Acta 455 (1976) 1.
[10] V. Kralj-Iglič, S. Svetina, B. Žekš, Eur. Biophys. J. 24 (1996) 311.
[11] J.N. Israelachvili, D.J. Mitchell, B.W. Ninham, J. Chem. Soc. Faraday Trans. 72 (1976) 1525.
[12] H. Heerklotz, H. Binder, G. Lantzsch, G. Klose, A. Blume, J. Phys. Chem. B 101 (1997) 639.
[13] M. Bobrowska-Hägerstrand, V. Kralj-Iglič, A. Iglič, K. Bialkowska, B. Isomaa, H. Hägerstrand, Biophys. J. 77 (1999) 3356.
[14] M.P. Sheetz, S.J. Singer, Natl. Acad. Sci. USA 71 (1974) 4457.
[15] E.A. Evans, Biophys. J. 14 (1974) 923.
[16] W. Helfrich, Z. Naturforsch. 28c (1973) 693.
[17] V. Kralj-Iglič, V. Heinrich, S. Svetina, B. Žekš, Eur. Phys. J. B 10 (1999) 5.
[18] V.S. Markin, Biophys. J. 36 (1981) 1.
[19] S. Leibler, J. Phys. 47 (1986) 507.
[20] D. Andelman, T. Kawakatsu, K. Kawasaki, Europhys. Lett. 19 (1992) 57.
[21] U. Seifert, Phys. Rev. Lett. 70 (1993) 1335.
[22] A.A. Boulbitch, Phys. Rev. E 56 (1997) 3395.
[23] J.B. Fournier, Phys. Rev. Lett. 76 (1996) 4436.
[24] S. Svetina, B. Žekš, in: D.D. Lasic, Y. Barenholz (Eds.), Handbook of Nonmedical Applications of Liposomes, CRC Press, Boca Raton, FL, 1996, p. 13.
[25] J. Gimsa, C. Ried, Mol. Membr. Biol. 12 (1995) 247.
[26] R. Glaser, Biophys. J. 75 (1998) 569.
[27] M.M. Gedde, D.K. Davis, W.H. Huestis, Biophys. J. 72 (1997) 1234.
[28] S. Svetina, B. Žekš, J. Theor. Biol. 146 (1990) 115.
[29] R. Lipowsky, Nature 349 (1991) 475.
[30] U. Seifert, Adv. Phys. 46 (1997) 13.
[31] A. Ben-Shaul, W.M. Gelbart, in: W.M. Gelbart, A. Ben-Shaul, D. Roux (Eds.), Micelles, Membranes, Microemulsions, and Monolayers, Springer-Verlag, New York, 1994.
[32] J. Gimsa, Biophys. J. 75 (1998) 568.
[33] M.M. Gedde, E. Yang, W.H. Huestis, Biochim. Biophys. Acta 1417 (1999) 2463.
[34] D.A. Berk, R. Hochmuth, Biophys. J. 61 (1992) 9.
[35] W.C. Hwang, R.E. Waugh, Biophys. J. 72 (1997) 2669.
[36] D.E. Discher, N. Mohandas, E. Evans, Science 266 (1994) 1032.
[37] H. Hägerstrand, V. Kralj-Iglič, M. Bobrowska-Hägerstrand, A. Iglič, Bull. Math. Biol. 61 (1999) 1019.
[38] E.A. Evans, R. Skalak, Mechanics and Thermodynamics of Biomembranes, CRC Press, Boca Raton, FL, 1980.
[39] W. Wiese, W. Harbich, W. Helfrich, J. Phys. Cond. Matter 4 (1992) 1647.
[40] L. Miao, U. Seifert, M. Wortis, H.G. Döbereiner, Phys. Rev. E 49 (1994) 5389.
[41] P.R. Zarda, S. Chien, R. Skalak, J. Biomech. 10 (1977) 211.
[42] B.T. Stokke, A. Mikkelsen, A. Elgsaeter, Eur. Biophys. J. 13 (1986) 219.
[43] E. Sackmann, FEBS Lett. 346 (1994) 3.
[44] A. Iglič, J. Biomech. 30 (1997) 35.
[45] A. Iglič, V. Kralj-Iglič, H. Hägerstrand, Eur. Biophys. J. 27 (1998) 335.
[46] K.H. Parker, C.P. Winlowe, Biophys. J. 77 (1999) 3096.
[47] G.R. Pasternack, R.A. Anderson, T.L. Leto, V.T. Marchesi, J. Biol. Chem. 260 (1985) 3676.
[48] A. Iglič, S. Svetina, B. Žekš, Biophys. J. 69 (1995) 274.
[49] P.S. Low, B.M. Willardson, N. Mohandas, M. Rossi, S. Shohet, Blood 77 (1991) 1581.
[50] M. Paulitschke, G.B. Nash, D.J. Anstee, M.J.A. Tanner, W.B. Gratzer, Blood 86 (1995) 342.
[51] T.M. Fischer, J. Phys. II France 2 (1992) 337.
[52] T.M. Fischer, J. Phys. II France 3 (1993) 1795.
[53] S. Chiruvolu, H.E. Warriner, E. Naranjo, K. Kraiser, S.H.J. Idziak, J. Radler, R.J. Plano, J.A. Zasadzinsky, C.R. Safinya, Science 266 (1994) 1222.
[54] V. Kralj-Iglič, A. Iglič, H. Hägerstrand, P. Peterlin, Phys. Rev. E 61 (2000) 4230.
[55] C.R. Safinya, Coll. Surf. A: Physicochem. Eng. Aspects 128 (1997) 183.
[56] J.F. Lennon, F. Brochard, J. Phys. (Paris) 36 (1975) 1035.
[57] D. Nelson, T. Piran (Eds.), Statistical Mechanics of Membranes and Surfaces, Jerusalem Winter School, World Scientific, Singapore, 1989.
[58] J. Prost, R. Bruinsma, Europhys. Lett. 33 (1996) 321.
[59] R. Netz, J. Phys. I (France) 7 (1997) 833.
[60] P.G. Dommersnes, J.B. Fournier, Europhys. Lett. 46 (1999) 256.
[61] S.T. Milner, S.A. Safran, Phys. Rev. Lett. 36 (1987) 4371.
[62] J. Majhenc, Observation of thermal fluctuations of phospholipid vesicles and determination of bending elastic constant of phospholipid membrane, M.Sc. Thesis, University of Ljubljana, Ljubljana, 1995.
[63] H.U. Lutz, A.J. Lomant, P. McMillan, E. Wehrli, J. Cell. Biol. 74 (1977) 389.
[64] J.M. Schnur, Science 262 (1993) 1669.